Synthesis, Magnetic Properties, and Electronic Spectra of Octahedral Mixed-Ligand (*β*-Diketonato)nickel(II) Complexes with a Chelated Nitronyl Nitroxide Radical

Takafumi Yoshida,[†] Takayoshi Suzuki,[†] Kan Kanamori,[‡] and Sumio Kaizaki*[,†]

Departments of Chemistry, Graduate School of Science, Osaka University, Toyonaka, Osaka 560-0045, Japan, and Faculty of Science, Toyama University, Gofuku, Toyama 930-0887, Japan

Received November 5, 1998

Two series of new mixed-ligand nitronyl nitroxide Ni(II) complexes of [Ni(*β*-diketonato)$_2$(NIT2-py)] and [Ni(*β*-diketonato)(tmen)(NIT2-py)]$^+$ types with various kinds of *β*-diketonates have been synthesized and structurally and magnetically characterized, where NIT2-py is 2-(2-pyridyl)-4,4,5,5-tetramethyl-4,5-dihydro-1*H*-imidazolyl-1-oxyl 3-oxide and tmen is *N*,*N*,*N*′,*N*′-tetramethylethylenediamine. The X-ray structural analysis for three tmen complexes with 2,4-pentanedionate (**1b**), 1,3-diphenyl-1,3-propanedionate (**2b**), and 4,4,4-trifluoro-1-phenyl-1,3-butanedionate (**5b**) demonstrated that the *β*-diketonato complexes assume a mer (cis,trans) N_3O_3 geometrical configuration. The structural parameters are as follows: **1b** ($C_{23}H_{39}F_6N_5NiPO_4 \cdot {}^1/_3CH_2Cl_2$), trigonal, $R\bar{3}$, a = 33.299(5) Å, c = 15.007(9) Å, Z = 18; **2b** ($C_{28}H_{41}F_6N_5NiPO_4$), orthorhombic, *Pbca*, a = 23.732(6) Å, b = 18.504(5) Å, c = 15.345(4) Å, Z = 8; **5b** ($C_{28}H_{38}F_9N_5NiPO_4$), triclinic, $P\bar{1}$, a = 12.068(2) Å, b = 16.942(2) Å, c = 9.161(1) Å, α = 105.26(1)°, β = 103.72(1)°, γ = 71.62(1)°, Z = 2. The antiferromagnetic interactions between Ni(II) and NIT2-py were found within ranges of J = −207 to −224 cm^{-1} for the bis(*β*-diketonato) complexes and of J = −35 to −150 cm^{-1} for the (*β*-diketonato)(tmen) complexes. The displacement of the *β*-diketonates with tmen in bis(*β*-diketonato) complexes decreases the J values, and the effect of the 1,3-substituents in the *β*-diketonates on the J values is observed in a systematic manner for all the bis(*β*-diketonato) complexes and for the (methyl- and phenyl-substituted-*β*-diketonato)(tmen) complexes but not for the trifluoromethyl-substituted complex. The room-temperature electronic spectra of the bis(*β*-diketonato) and the (*β*-diketonato)(tmen) complexes exhibit enhanced spin-forbidden d−d transitions at 13.0 × 10^3 cm^{-1} and new metal−ligand charge-transfer (MLCT) transitions around (16.0−19.0) × 10^3 cm^{-1}. The variation of the spectroscopic characteristics with modification of the *β*-diketonato ligands is discussed through the exchange mechanism in connection with the antiferromagnetic interactions in terms of the substituent effects or the Hammett σ_m constants.

Introduction

Recently, there have been a number of studies on multi-spin exchange coupled systems consisting of paramagnetic metal ions and nitronyl nitroxide radicals such as several derivatives of 4,4,5,5-tetramethyl-4,5-dihydro-1*H*-imidazolyl-1-oxyl 3-oxide (NIT).[1−8] They have been concerned mainly with magnetic properties leading to molecular ferromagnetism.[1] Only a limited number of the coligands such as hexafluoroacetylacetonate (hfac) and chloride have been adopted,[6] which were claimed to increase the Lewis acidity of central metal ions[9] so that NIT derivatives as weak Lewis bases[10] were more susceptible to coordination through an NIT-py *N*-O oxygen. Therefore, the magnetic properties have been compared only among different types of complexes so far, but they have not been examined in terms of the coligand effect for the same types. If chelated NIT2-py (2-(2-pyridyl)-4,4,5,5-tetramethyl-4,5-dihydro-1*H*-imidazolyl-1-oxyl 3-oxide) radical metal complexes with various kinds of *β*-diketonates (Chart 1) were available, a variation of *β*-diketonato coligands could afford modification of the Lewis acidity of a metal ion center, which would provide more invaluable

Chart 1

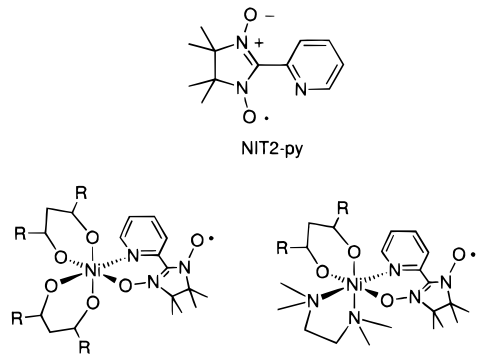

[†] Osaka University.
[‡] Toyama University.

(1) Caneschi, A.; Gatteschi, D.; Rey, P. *Prog. Inorg. Chem.* **1991**, *39*, 331.
(2) Caneschi, A.; Gatteschi, D.; Laugier, J.; Rey, P. *J. Am. Chem. Soc.* **1987**, *109*, 2191.
(3) Laugier, J.; Rey, P.; Benelli, C.; Gatteschi, D.; Zanchini, C. *J. Am. Chem. Soc.* **1986**, *108*, 6931.
(4) Caneschi, A.; Gatteschi, D.; Laugier, J.; Rey, P.; Sessoli, R. *Inorg. Chem.* **1988**, *27*, 1553.
(5) Caneschi, A.; Gatteschi, D.; Renaed, J. P.; Rey, P.; Sessoli, R. *Inorg. Chem.* **1989**, *28*, 2940.
(6) Luneau, D.; Risoan, G.; Rey, P.; Grand, A.; Caneschi, A.; Gatteschi, D.; Laugier, J. *Inorg. Chem.* **1993**, *32*, 5616.
(7) Luneau, D.; Laugier, J.; Rey, P.; Ulrich, G.; Ziessel, R.; Legoll, P.; Drillon, M. *J. Chem. Soc., Chem. Commun.* **1994**, 741.
(8) Romero, F. M.; Luneau, D.; Ziessel, R. *J. Chem. Soc., Chem. Commun.* **1998**, 551.
(9) Parentheimer, W.; Drago, R. S. *Inorg. Chem.* **1970**, *1*, 47.
(10) Zelonka, R. A.; Baird, M. C. *J. Am. Chem. Soc.* **1971**, *93*, 6066.

10.1021/ic981283n CCC: $18.00
Published on Web 02/27/1999

information not only on the spectroscopic behavior as our main interest but also on the magnetic interactions between paramagnetic metal ions and NIT2-py.

A number of investigations[6,11−20] on electronic spectra of multi-spin exchange coupled systems of transition metal complexes having binuclear structures or containing radical ligands have been published. Strongly spin-coupled Cr(III) semiquinone or phenoxy radical complexes[19,20] have demonstrated large intensity enhancement of the spin forbidden d−d transitions arising from strong antiferromagnetic interactions. In these cases, the magnetic interactions are so strong that they exhibit temperature-independent magnetic moments. In [Ni(hfac)$_2$(NIT2-py)] as reported previously,[6] on the other hand, the magnetic interactions are found to be not so strong. Such a moderately spin-coupled system is expected to show some quantitative relations between the intensity enhancement and the magnetic exchange interaction, which have seldom been examined. For this purpose, we have begun a systematic study on Ni(II) complexes containing a NIT2-py radical and various kinds of β-diketonato coligands. A preliminary communication has already been published regarding some bis(β-diketonato) nickel(II) complexes along with paramagnetic chromium(III) ions.[21]

In this paper, the synthesis and characterization of two series of mixed-ligand NIT2-py nickel(II) complexes of [Ni(β-diketonato)$_2$(NIT2-py)] and [Ni(β-diketonato)(tmen)(NIT2-py)]$^+$ (tmen = *N,N,N′,N′*-tetramethylethylenediamine) types with various kinds of β-diketonate ligands will be reported. The magnetic properties and the electronic absorption spectra of these NIT2-py nickel(II) complexes will be examined in connection with the coligand (substituent) effect or the variation of β-diketonato ligands. They are expected to be appropriate candidates for finding a relationship between the spectral properties and the exchange interactions with variation of the β-diketonate coligands leading to fine-tuning of the spin-coupled systems.

Experimental Section

Ligands. The radical ligand NIT2-py was prepared by the literature method.[22] The β-diketonates used (β-diketonato = acac (2,4-pentanedionato), bzac (1-phenyl-1,3-butanedionato), dbm (1,3-diphenyl-1,3-propanedionato), tfac(1,1,1-trifluoro-2,4-pentanedionato), hfac (1,1,1,5,5,5-hexafluoro-2,4-pentanedionato)) were commercially available.

Syntheses of the Starting and Reference Complexes. (i) Starting Complexes for Bis(β-diketonato)nickel(II) Compounds. [Ni(β-diketonato)$_2$(H$_2$O)$_2$] complexes were synthesized according to the literature methods.[23,24]

(ii) Starting Complexes for Mono(β-diketonato)nickel(II) Compounds. [Ni(β-diketonato)(tmen)]PF$_6$ (β-diketonato = acac, bzac, dbm) and [Ni(β-diketonato)(NO$_3$)(tmen)] (β-diketonato = tfac, bztfac (4,4,4-trifluoro-1-phenyl-1,3-butanedionato), nptfac (4,4,4-trifluoro-1-(2-naphthyl)-1,3-butanedionato)) complexes were synthesized according to the method of Fukuda et al.[25−27]

(iii) Reference Complexes. [Ni(β-diketonato)$_2$(tmen)] (β-diketonato = acac (**1c**), bzac (**2c**), dbm (**3c**), tfac (**4c**), hfac (**5c**)) complexes were synthesized according to the literature methods,[25−28] and [Ni(β-diketonato)(NO$_3$)(tmen)] (β-diketonato = acac (**1d**), bzac (**2d**), dbm (**3d**), tfac (**4d**), bztfac (**5d**), nptfac (**6d**)) complexes were used as the reference complexes for spectral measurements.

Syntheses of the NIT2-py Complexes. (i) [Ni(acac)$_2$(NIT2-py)] (1a). To a solution of 0.29 g (1 mmol) of [Ni(acac)$_2$(H$_2$O)$_2$] in 30 mL of CH$_2$Cl$_2$ was slowly added a solution of 0.24 g (1 mmol) of NIT2-py in 30 mL of CH$_2$Cl$_2$ with stirring at room temperature for 12 h. The color of the solution changed to dark green. After this solution was condensed to dryness, the residue was dissolved in CH$_2$Cl$_2$. The crude product, obtained by adding *n*-heptane, was filtered off. The dark green powder of [Ni(acac)$_2$(NIT2-py)] was recrystallized from CH$_2$Cl$_2$−*n*-heptane. The yield was 0.31 g (54.4%).

The other bis(β-diketonato) complexes [Ni(β-diketonato)$_2$(NIT2-py)] (β-diketonato = bzac (**2a**), dbm (**3a**), tfac (**4a**), hfac (**5a**)) were obtained by the same method as that for the acac complex (**1a**).

(ii) [Ni(acac)(tmen)(NIT2-py)]PF$_6$ (1b). To a solution of 0.42 g (1 mmol) of [Ni(acac)(tmen)]PF$_6$ in 30 mL of CH$_2$Cl$_2$ was slowly added a solution of 0.24 g (1 mmol) of NIT2-py in 30 mL of CH$_2$Cl$_2$ with stirring at room temperature for 30 min. The color of the solution changed to dark green. The solution was evaporated under reduced pressure. The crude product, obtained by adding ether, was filtered off. Dark green crystals of [Ni(acac)(tmen)(NIT2-py)]PF$_6$·$^1/_3$CH$_2$Cl$_2$ were recrystallized from CH$_2$Cl$_2$−ether. The yield was 0.59 g (90.9%).

The other (β-diketonato)(tmen) complexes [Ni(β-diketonato)(tmen)(NIT2-py)]PF$_6$ (β-diketonato = bzac (**2b**), dbm (**3b**)) were obtained by the same method as that for the acac complex. The remaining complexes with tfac (**4b**), bztfac (**5b**), and nptfac (**6b**) were synthesized with the use of [Ni(β-diketonato)(NO$_3$)(tmen)] complexes.

X-ray Structural Analysis. Dark green crystals of **1b**, **2b**, and **5b** suitable for X-ray crystal analyses were obtained by a diffusion technique using dichloromethane solutions and ether. The crystal of **1b** was mounted in a glass capillary. The crystals of **2b** and **5b** were glued atop a glass fiber. The X-ray intensities were measured at 23 °C with graphite-monochromated Mo Kα radiation (λ = 0.710 73 Å) on a Rigaku AFC-5R four-circle diffractometer using the $\omega-2\theta$ scan technique. The structure was solved by direct methods and expanded using Fourier techniques. The structure could be solved reasonably by the usual heavy-atom method using the SHELXS-86 program.[29] The positions of hydrogen atoms were obtained by subsequent Fourier-difference syntheses. The function, $\sum w(|F_o| - |F_c|)^2$ where $w^{-1} = \sigma^2(F_o) + (0.00022|F_o|)^2$, was minimized (refined on F) by the full-matrix least-squares method using anisotropic and isotropic thermal parameters for all non-hydrogen and hydrogen atoms, respectively. The non-hydrogen atoms were refined anisotropically. All hydrogen atoms except for those of the dichloromethane of crystallization were introduced in calculated positions, and the thermal parameters were refined isotropically. Complex neutral-atom scattering factors were used.[30] All calculations were carried out on an SGI Indy workstation using TEXSAN software.[31]

Magnetic Susceptibilities. Magnetic susceptibility data were measured at 1000 Oe between 2 and 300 K by using a SQUID suscep-

(11) Güdel, H. U. In *Magnetic-Structural Correlations in Exchange Coupled Systems*; Willet, R. D., Gatteschi, D., Kahn, O., Eds.; Reidel: Dordrecht, The Netherlands, 1985; p 297.
(12) McCarthy, P. U.; Güdel, H. U. *Coord. Chem. Rev.* **1988**, *88*, 69.
(13) Bellitto, C.; Day, P. *J. Chem. Soc., Dalton Trans.* **1978**, 1207.
(14) Bellitto, C.; Day, P. *J. Chem. Soc., Dalton Trans.* **1986**, 847.
(15) Bellitto, C.; Day, P. *J. Mater. Chem.* **1992**, *2*, 265.
(16) Mathonieres, C.; Kahn, O.; Daran, J. C.; Hilbig, H.; Kohler, F. H. *Inorg. Chem.* **1993**, *32*, 4057.
(17) Mathonieres, C.; Kahn, O. *Inorg. Chem.* **1994**, *33*, 2103.
(18) Cador, C.; Mathonieres, C.; Kahn, O. *Inorg. Chem.* **1997**, *36*, 1923.
(19) Benelli, C.; Dei, A.; Gatteschi, D.; Gudel, H. U.; Pardi, L. *Inorg. Chem.* **1989**, *28*, 3089.
(20) Sokolowski, A.; Bothe, E.; Bill, E.; Weyhermuller, T.; Wieghardt, K. *J. Chem. Soc., Chem. Commun.* **1996**, 1671.
(21) Yoshida, T.; Kanamori, K.; Takamizawa, S.; Mori, W.; Kaizaki, S. *Chem. Lett.* **1997**, 603.
(22) Ullman, E. F.; Osiecki, J. H.; Rey, P.; Sessoli, R. *J. Am. Chem. Soc.* **1972**, *94*, 7049.
(23) Charles, R. G.; Pawlikowsky, M. A. *J. Phys. Chem.* **1958**, *62*, 440.
(24) Nakamoto, K.; McCarthy, P. J.; Martell, A. E. *Nature* **1959**, *183*, 459.
(25) Fukuda, Y.; Sone, K. *Bull. Chem. Soc. Jpn.* **1970**, *43*, 2282.
(26) Fukuda, Y.; Sone, K. *J. Inorg. Nucl. Chem.* **1972**, *34*, 2315.
(27) Fukuda, Y.; Sone, K. *J. Inorg. Nucl. Chem.* **1975**, *37*, 455.
(28) Yoshida, T.; Oguni, M.; Mori, Y.; Fukuda, Y. *Solid State Commun.* **1995**, 93, 159.
(29) Sheldrick, G. M. SHELXS-86: Program for Crystal Structure Determination. University of Göttingen, Germany, 1986.
(30) Cromer, D. T.; Waber, J. T. *International Tables for X-ray Crystallography*; Kynoch Press: Birmingham, England, 1974; Vol. 4.
(31) *TEXSAN: Single-Crystal Structure Analysis Software*, Ver. 1.7; Molecular Structure Corp.: The Woodlands, TX, 1995.

Table 1. Elemental Analyses of the Radical Complexes

compound		% found (calcd)		
		C	H	N
1a	$[Ni(acac)_2(NIT2\text{-}py)]\cdot CH_2Cl_2$	48.11 (47.95)	5.65 (5.60)	7.45 (7.29)
2a	$[Ni(bzac)_2(NIT2\text{-}py)]$	62.40 (62.46)	5.53 (5.57)	6.96 (6.83)
3a	$[Ni(dbm)_2(NIT2\text{-}py)]$	66.45 (68.22)	5.23 (5.18)	5.70 (5.68)
4a	$[Ni(tfac)_2(NIT2\text{-}py)]$	44.41 (44.10)	3.99 (4.04)	7.27 (7.01)
1b	$[Ni(acac)(tmen)(NIT2\text{-}py)]\text{-}PF_6\cdot{}^1/_3CH_2Cl_2$	41.54 (41.13)	5.87 (5.87)	10.34 (10.28)
2b	$[Ni(bzac)(tmen)(NIT2\text{-}py)]PF_6$	47.08 (47.02)	5.64 (5.78)	9.79 (9.79)
3b	$[Ni(dbm)(tmen)(NIT2\text{-}py)]PF_6$	51.15 (50.99)	5.50 (5.58)	8.93 (9.01)
4b	$[Ni(tfac)(tmen)(NIT2\text{-}py)]PF_6$	39.55 (39.06)	5.16 (5.13)	9.89 (9.90)
5b	$[Ni(bztfac)(tmen)(NIT2\text{-}py)]PF_6$	43.67 (43.72)	4.85 (4.98)	9.08 (9.10)
6b	$[Ni(nptfac)(tmen)(NIT2\text{-}py)]PF_6$	47.01 (46.91)	4.91 (4.92)	8.63 (8.55)

tometer (MPMS-5S, Quantum Design). Pascal's constants were used to determine the constituent atom diamagnetism.

Spectral Measurements. UV−visible spectra were recorded in CH_2Cl_2 by a Perkin-Elmer Lambda 19 spectrophotometer at room temperature. Low-temperature UV−visible spectrum was measured at 77 K by the same spectrophotometer with an Oxford Cryostat DN1704 (static) in a film made from methacrylic acid methyl ester. Magnetic circular dichroism (MCD) spectra in CH_2Cl_2 were obtained in a magnetic field of 1.5 T (1 T = 1.0×10^4 G) with a Jasco J-720W spectropolarimeter at room temperature. Resonance Raman spectra were measured in the solid state by a Jasco NR1800 spectrophotometer at room temperature using Ar laser lines (488.00, 514.50 nm), the He−Ne laser line (632.80 nm), and dye laser lines (R6G, 581.09, 594.85, 617.17 nm; DCM, 668.85, 698.08 nm) as excitation sources.

Results and Discussion

1. Preparations and Characterization. The [Ni(β-diketonato)$_2$(NIT2-py)] complexes were newly obtained from the corresponding bis(β-diketonato)diaqua nickel(II) complexes in CH_2Cl_2 by the modified method for the hfac complex[6] and recrystallized from CH_2Cl_2 and *n*-heptane. The satisfactory elemental analyses confirm the expected chemical formulas for these complexes as shown in Table 1. The visible absorption spectral patterns[21] of [Ni(β-diketonato)$_2$(NIT2-py)] are similar to those of [Ni(hfac)$_2$(NIT2-py)], which was characterized by X-ray structural analysis[6] as having an NIT2-py chelate coordinated through the oxygen of the nitronyl nitroxide group and the pyridyl nitrogen. Therefore, these complexes have a chelated NIT2-py along with two β-diketonate chelates. For asymmetric tfac and bzac ligands, there are three geometrical isomers. However, the existence of three isomers could not be confirmed even by ^{1}H and ^{2}H NMR spectra.[32] New types of mixed-ligand complexes [Ni(β-diketonato)(tmen)(NIT2-py)]PF_6 were synthesized from the corresponding [Ni(β-diketonato)(tmen)]PF_6 or [Ni(β-diketonato)(NO_3)(tmen)] complexes. They give satisfactory elemental analyses as shown in Table 1. The absorption spectra are characteristic of the chelated NIT2-py complexes as observed similarly for the bis(β-diketonato)(NIT2-py) complexes.[6,21] It is noted that the β-diketonato complexes other than that of hfac can be obtained against the previous notion[6,10] that electrophilic acid metal centers such as the hfac complex are favorable partners for nitroxides. These new Ni(II) complexes are air-stable in CH_2Cl_2 at room temperature for a few weeks. Three of these mixed-ligand (tmen) complexes were determined by X-ray analysis to assume a mer (cis,trans) geometrical structure with a chelated NIT2-py, as discussed below.

2. Molecular Structure. Crystallographic data for [Ni(acac)(tmen)(NIT2-py)]$PF_6\cdot{}^1/_3CH_2Cl_2$ (**1b**), [Ni(bzac)(tmen)(NIT2-py)]PF_6 (**2b**), and [Ni(bztfac)(tmen)(NIT2-py)]PF_6 (**5b**) are listed in Table 2. Selected bond distances, bond angles, torsion angles, and dihedral angles are summarized in Table 3.

Table 2. Crystallographic Data for **1b**, **2b**, and **5b**

	1b	**2b**	**5b**
formula	$C_{23}H_{39}F_6N_5NiPO_4\cdot{}^1/_3CH_2Cl_2$	$C_{28}H_{41}F_6N_5NiPO_4$	$C_{28}H_{38}F_9N_5NiPO_4$
fw	681.65	715.33	769.30
crystal system	trigonal	orthorhombic	triclinic
space group	$R\bar{3}$ (No. 148)	*Pbca* (No. 61)	$P\bar{1}$ (No. 2)
a, Å	33.299(5)	23.732(6)	12.068(2)
b, Å		18.504(5)	16.942(2)
c, Å	15.007(9)	15.345(4)	9.161(1)
α, deg			105.26(1)
β, deg			103.72(1)
γ, deg			71.62(1)
V, Å^3	14411(8)	6738(2)	1690.3(5)
Z	18	8	2
ρ_{calcd}, g cm^{-3}	1.414	1.410	1.511
μ(Mo Kα), cm^{-1}	7.82	6.96	7.12
R^a	0.062	0.0562	0.055
$R_w{}^b$	0.062	0.0626	0.079

^{a} $R = \sum||F_o| - |F_c||/\sum|F_o|$. ^{b} $R_w = [\sum w(|F_o| - |F_c|)^2/\sum w|F_o|^2]^{1/2}$; $w^{-1} = \sigma_c^2(F_o) + (0.00022|F_o|)^2$.

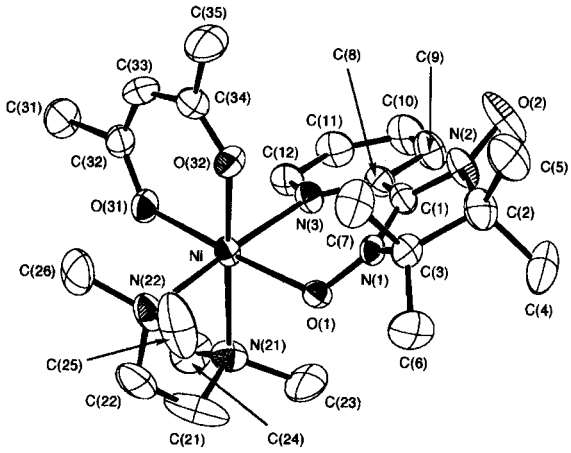

Figure 1. Molecular structure of [Ni(acac)(tmen)(NIT2-py)]$PF_6\cdot{}^1/_3CH_2Cl_2$ (**1b**).

The molecular structures of **1b**, **2b**, and **5b** are shown in Figures 1−3. They are distorted octahedral complexes which are chelated by the pyridyl nitrogen and nitronyl nitroxide oxygen of NIT2-py and each of the β-diketonato ligands and tmen (**1b**, **2b**, **5b**). Each β-diketonato complex assumes a mer (cis,trans) geometrical structure in such a way that the *N*-O oxygen of NIT binds trans to the β-diketonato oxygen and that the pyridyl nitrogen is located at the trans position of the tmen amine nitrogen. A molecular model consideration suggests that a steric congestion between the pyridyl group of NIT2-py and one of the *N*-methyl groups of tmen prevents the formation of

(32) Yoshida, T.; Kaizaki, S. *Inorg. Chem.* **1999**, *38*, 1054.

Table 3. Selected Bond Distances (Å), Bond Angles (deg), Torsion Angles (deg), and Dihedral Angles (deg) of **1b**, **2b**, and **5b**

	1b	2b	5b
	Bond Distances		
Ni−O(1)	2.052(4)	2.055(4)	2.056(2)
Ni−O(31)	1.993(4)	1.998(4)	2.021(2)
Ni−O(32)	1.993(5)	2.020(4)	2.025(2)
Ni−N(3)	2.144(5)	2.123(5)	2.139(2)
Ni−N(21)	2.171(6)	2.168(6)	2.171(2)
Ni−N(22)	2.170(6)	2.144(6)	2.154(3)
O(1)−N(1)	1.286(6)	1.289(6)	1.292(3)
O(2)−N(2)	1.257(7)	1.277(8)	1.270(3)
N(1)−C(1)	1.336(8)	1.343(8)	1.331(3)
N(2)−C(2)	1.352(8)	1.355(9)	1.354(3)
N(3)−C(8)	1.340(8)	1.355(8)	1.354(3)
N(3)−C(12)	1.361(8)	1.340(8)	1.344(4)
C(1)−C(8)	1.471(9)	1.463(9)	1.466(4)
	Bond Angles		
O(1)−Ni−O(31)	176.6(2)	176.2(2)	176.48(8)
O(1)−Ni−O(32)	87.7(2)	88.3(2)	88.46(8)
O(1)−Ni−N(3)	85.4(2)	85.5(2)	85.81(8)
O(1)−Ni−N(21)	87.0(2)	88.8(2)	88.67(9)
O(1)−Ni−N(22)	92.4(2)	92.6(2)	92.59(9)
O(31)−Ni−O(32)	92.0(2)	91.5(2)	90.54(8)
O(31)−Ni−N(3)	91.2(2)	90.6(2)	90.76(8)
O(31)−Ni−N(21)	93.5(2)	91.6(2)	92.49(9)
O(31)−Ni−N(22)	91.0(2)	91.3(2)	90.84(9)
O(32)−Ni−N(3)	89.2(2)	86.0(2)	86.66(9)
O(32)−Ni−N(21)	173.7(2)	176.1(2)	175.85(9)
O(32)−Ni−N(22)	93.2(2)	93.3(2)	92.88(9)
N(3)−Ni−N(21)	93.9(2)	96.3(2)	96.13(9)
N(3)−Ni−N(22)	176.7(2)	178.0(2)	178.34(9)
N(21)−Ni−N(22)	83.6(2)	84.3(2)	84.2(1)
Ni−O(1)−N(1)	118.9(3)	117.9(3)	117.8(2)
O(1)−N(1)−C(1)	127.6(5)	125.3(5)	126.3(2)
O(2)−N(2)−C(1)	126.5(7)	125.6(7)	126.4(3)
Ni−N(3)−C(8)	126.3(4)	124.7(4)	123.9(2)
Ni−N(3)−C(12)	116.2(4)	118.8(4)	119.6(2)
	Torsion Angles		
N(1)−C(1)−C(8)−N(3)	24(1)	25(1)	28.7(4)
N(21)−C(21)−C(22)−N(22)	−50(2)	−22(2)	−39(2)
	Dihedral Angles		
plane 1[a] vs plane 2[b]	23.15	23.68	28.69
plane 1 vs plane 3[c]	37.25	44.08	43.44
plane 2 vs plane 3	24.12	27.83	28.01

[a] Plane 1: O(1), N(1), C(1), N(2), O(2). [b] Plane 2: N(3), C(8), C(9), C(10), C(11), C(12). [c] Plane 3: O(1), O(31), N(3), N(22).

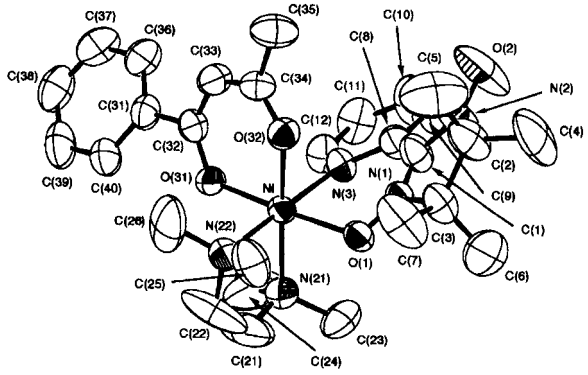

Figure 2. Molecular structure of [Ni(bzac)(tmen)(NIT2-py)]PF_6 (**2b**).

a fac (cis,cis) configuration. Therefore, the mer isomer seems to be stereoselectively formed. Since the bzac and bztfac ligands are asymmetric, there are two possible isomers in a mer mode with respect to the coordination of the tmen nitrogen or NIT2-py oxygen trans to the benzoyl oxygen in the bzac and bztfac ligands. The X-ray analysis revealed that the *N*-O oxygen of NIT2-py binds at the trans position of the benzoyl group in the

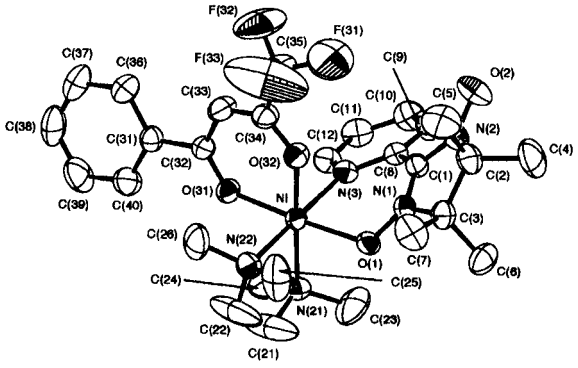

Figure 3. Molecular structure of [Ni(bztfac)(tmen)(NIT2-py)]PF_6 (**5b**).

bzac and bztfac complexes as shown in Figures 2 and 3. The Ni−O(1) bond lengths of **1b**, **2b**, and **5b** are in a range from 2.052 to 2.056 Å while the Ni−N(3) lengths range from 2.144 to 2.123 Å, respectively. They are longer than the corresponding Ni−O (2.029(2) Å) and Ni−N (2.073(3) Å) lengths of the bis(hfac) complex.[6] Since there is no variation of the bond lengths despite the expected difference in Lewis basicity of the β-diketonates, such a significant bond elongation may result from the steric congestion due to the bulkier tmen coordination compared with that of hfac in the bis(hfac) complex but not from the weaker Lewis base β-diketonate coordination which could bring the central nickel ion into weaker Lewis acids. The N(1)−O(1) (coordinated) bond lengths of the nitronyl nitroxide radical moiety are 1.286(6), 1.289(6), and 1.292(3) Å, and the N(2)−O(2) (uncoordinated) ones are 1.257(7), 1.277(8), and 1.270(3) Å, respectively, for **1b**, **2b**, and **5b**, compared with the corresponding N(2)−O(5) (1.287(4) Å) and N(3)−O(6) (1.265(5) Å) lengths for the bis(hfac) complex,[6] indicating the existence of the nitronyl nitroxide radical on complexation. The O(1)−Ni−N(3) and Ni−O(1)−N(1) bond angles are 85.4(2), 85.5(2), 85.81(8)° and 118.9(3), 117.9(3), 117.8(2)°, respectively, for **1b**, **2b**, and **5b**. The former and latter angles are smaller and larger than the corresponding O(5)−Ni−N(1) (86.3(1)°) and Ni−O(5)−N(2) (115.4(2)°) angles, respectively, of the bis(hfac) complex.[6] This may be due to the bulkier tmen coordination as mentioned above.

As shown in Table 3, the dihedral angles between planes 1 and 3 (the radical (O(1), N(1), C(1), N(2), O(2)) and the coordination (O(1), O(31), N(3), N(22)) planes, respectively) are much larger than those of the analogous tetradentate biradical complexes.[8] The conformation of the six-membered NIT2-py chelate ring around the Ni(II) ion is a kind of envelope, where the plane (Ni, N(3), C(8), C(1)) is nearly planar. Taking into consideration the torsion angles of N(1)−C(1)-C(8)−N(3) for NIT2-py and N(21)−C(21)-C(22)−N(22) for the tmen for **1b**, **2b**, and **5b**, these complexes with a Λ absolute configuration arising from three chelates around a Ni(II) ion assume the δ(lel) (NIT2-py) and λ(ob) (tmen) conformations and vice versa according to the definition for chelate ring chirality based on a pair of skew lines consisting of the N(3)−C(8) and C(1)−N(1) bonds for NIT2-py and the N(21)−N(22) and C(21)−C(22) bonds for tmen in terms of IUPAC nomenclature.[33]

3. Magnetic Properties. The temperature dependences of the magnetic susceptibilities (χ_M) in the form of $\chi_M T$ vs T for [Ni(acac)$_2$(NIT2-py)]·CH_2Cl_2 (**1a**) and [Ni(acac)(tmen)(NIT2-py)]-PF_6·$^1/_3CH_2Cl_2$ (**1b**) are shown in Figure 4. The coupling constants J involving a nickel(II) ion and NIT2-py were obtained

(33) *Nomenclature of Inorganic Chemistry, Recommendations 1990*; Leigh, G. J., Ed.; Blackwell Scientific Publications: London, 1990.

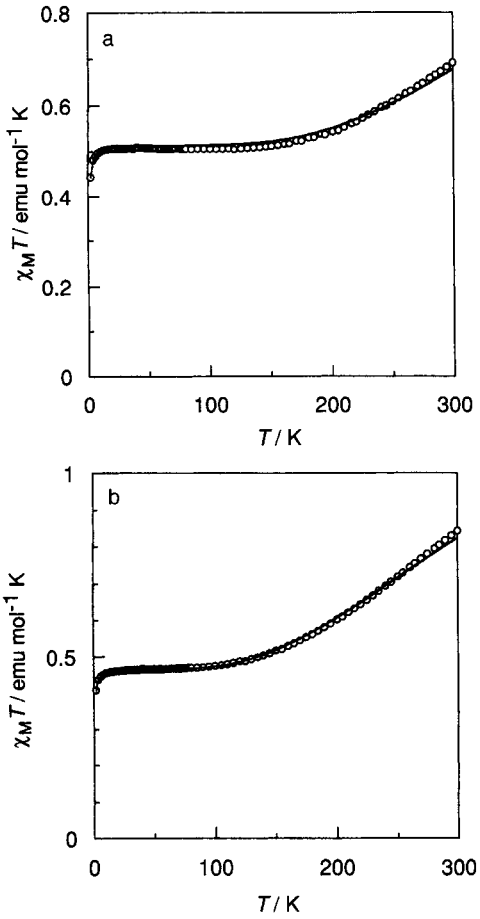

Figure 4. Temperature dependence of the magnetic susceptibilities for **1a** (a) and **1b** (b) in the form of $\chi_M T$ vs T. The solid line is calculated for the two-spin system.

Table 4. Magnetic Parameters for the Radical Complexes

compound	g	J^a cm^{-1}	θ, K	$10^{-6}R^b$
1a [Ni(acac)$_2$(NIT2-py)]·CH_2Cl_2	2.34	−219.4	−0.323	15.6
2a [Ni(bzac)$_2$(NIT2-py)]	2.38	−223.8	−0.185	16.6
3a [Ni(dbm)$_2$(NIT2-py)]	2.06	−206.5	−0.114	12.5
4a [Ni(tfac)$_2$(NIT2-py)]	2.24	−207.6	−0.236	6.02
[Ni(hfac)$_2$(NIT2-py)][c]	2.268	−167		
1b [Ni(acac)(tmen)(NIT2-py)]PF_6·$^1/_3CH_2Cl_2$	2.23	−149.0	−0.298	1.60
2b [Ni(bzac)(tmen)(NIT2-py)]PF_6	2.24	−110.1	−0.001	4.89
3b [Ni(dbm)(tmen)(NIT2-py)]PF_6	2.25	−35.5	−0.579	10.3
4b [Ni(tfac)(tmen)(NIT2-py)]PF_6	2.29	−145.4	−0.460	10.0
5b [Ni(bztfac)(tmen)(NIT2-py)]PF_6	2.25	−99.8	−0.132	3.57
6b [Ni(nptfac)(tmen)(NIT2-py)]PF_6	2.26	−103.3	−0.103	4.38

[a] $H = -2JS_i \cdot S_j$. [b] $R = \sum(\chi_{obsd} - \chi_{calcd})^2/\sum(\chi_{obsd})^2$. [c] Reference 6.

by fitting the magnetic susceptibilities to a two-spin system as has been employed for the bis(hfac) complex by using a formula for the two-spin system ($S_1 = 1$, $S_2 = {}^1/_2$)[34] including the Weiss constant θ. The best fits give antiferromagnetic coupling constants J as summarized together with g and R values in Table 4. The Weiss constant θ is much smaller compared with the intramolecular one (J). A range of $J = -207$ to -224 cm^{-1} for the bis(β-diketonato) complexes is compared with the previously reported value (-167 cm^{-1}) for the bis(hfac) complex.[6] The observation of large antiferromagnetic interactions ($|J| > 200$ cm^{-1}) is not in line with the previous assumption that the chelation of NIT2-py may lead to a decrease in the intramolecular antiferromagnetic interaction.[6] On the other hand, the J values for the tmen complexes ranging from -35 to -150 cm^{-1} are smaller than those of the [Ni(β-diketonato)$_2$(NIT2-py)] complexes. This may arise from elongation of the coordination bond with NIT2-py around the Ni(II) ion in the tmen complexes as described above by the X-ray analysis. The following facts are also noted in connection with the X-ray structural parameters: the larger the absolute J values for **1b**, **2b**, and **5b**, the closer to 120° are the Ni−O(1)−N(1) angles and the shorter are the Ni−O(1) and O(1)−N(1) bond lengths. Nevertheless, deviation from orthogonality between the π^* SOMO of NIT2-py and the e_g(d) magnetic orbital of Ni(II) does not always result in the magnification of the J values as seen from the dihedral angles between planes 2 and 3 (vide supra). Observation of such a large range of the J values for the Ni(II) complexes with various kinds of the β-diketonates prompts us to evaluate the substituent effect or how the J values are influenced by variation of the β-diketonate coligands. This subject will be discussed in more detail with relation to the spectroscopic behavior in the section 7.

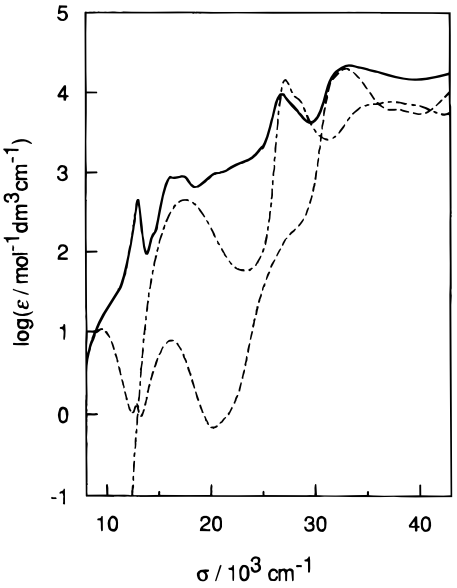

Figure 5. Absorption spectra of [Ni(acac)$_2$(NIT2-py)] (**1a**) (—), [Ni(acac)$_2$(tmen)] (**1c**) (- - -), and NIT2-py (— - —) in CH_2Cl_2.

4. UV Absorption Spectra. Absorption spectra of [Ni(acac)$_2$(NIT2-py)] and [Ni(acac)(tmen)(NIT2-py)]$^+$ are compared with those of NIT2-py and the nonradical complexes as shown in Figures 5 and 6. The numerical data including those for the corresponding nonradical β-diketonato complexes are summarized in Table 5. The absorption bands of NIT2-py at 17.8 $\times$ 10^3 and 27.4 $\times$ 10^3 cm^{-1} are assigned to the intraligand n−π^* and $\pi-\pi^*$ transitions, respectively.[35] The absorption bands of [Ni(β-diketonato)$_2$(NIT2-py)] complexes around 27 $\times$ 10^3 cm^{-1} correspond to the $\pi-\pi^*$ transitions of NIT2-py in view of the similarity in position and intensity with the exception of the [Ni(dbm)$_2$(NIT2-py)] band, for which the absorption intensity is larger than that for the other β-diketonato complexes due to the overlap with the phenyl $\pi-\pi^*$ transition in the dbm ligand. Since the higher frequency absorption band of [Ni(acac)$_2$(NIT2-py)] at 33.3 $\times$ 10^3 cm^{-1} is analogous in position and intensity to that of [Ni(acac)$_2$(tmen)] at 33.3 $\times$ 10^3 cm^{-1}, this is assigned to the $\pi-\pi^*$ transition or the charge transfer originating from the acetylacetonato ligand. From the similarity in UV spectral patterns between the NIT2-py complexes and the corresponding

(34) Wojciechowski, W. *Inorg. Chim. Acta* **1967**, *1*, 324.

(35) Osiecki, J. H.; Ullman, E. F. *J. Am. Chem. Soc.* **1969**, *90*, 1078.

Table 5. Absorption Spectral Data for NIT2-py, [Ni(β-diketonato)$_2$(NIT2-py)], [Ni(β-diketonato)(tmen)(NIT2-py)]$^+$, and [Ni(acac)$_2$(tmen)] in CH_2Cl_2

compound	σ_{max}, 10^3 cm^{-1} (ϵ, mol^{-1} dm^3 cm^{-1})						
NIT2-py	17.5 (450)	27.2 (14 300)	28.4^{sh} (8320)	35.1^{sh} (6940)	37.2 (7690)	39.9^{sh} (6860)	
1a	9.80^{sh} (17.1) 31.9^{sh} (17 100)	13.0 (448) 33.3 (21 500)	14.5^{sh} (167)	16.2 (872)	17.4 (894)	20.4^{sh} (963)	26.8 (9590)
2a	9.80^{sh} (18.7) 29.8 (23 900)	13.0 (465) 36.0 (20 000)	14.5^{sh} (154) 41.0 (31 000)	16.1 (870)	17.4 (881)	20.5 (1050)	26.9^{sh} (14 200)
3a	9.80^{sh} (29.5) 34.7^{sh} (38 900)	13.0 (472) 40.0 (21 400)	14.4^{sh} (147)	16.1 (894)	17.4 (908)	20.4 (1140)	27.1 (38 800)
4a	10.0 (14.6) 26.9 (10 700)	13.2 (258) 33.1 (19 000)	14.6^{sh} (133) 37.0 (15 100)	16.3 (583)	17.6 (657)	21.4^{sh} (757)	23.6^{sh} (1560)
5a	9.76 (14.5) 26.9 (10 800)	13.2 (111) 32.5 (16 200)	14.5^{sh} (107) 41.3^{sh} (12 800)	16.2 (417)	17.7 (502)	20.6^{sh} (325)	22.1^{sh} (600)
1b	10.2^{sh} (20.6) 3.15^{sh} (9940)	12.7 (278) 33.0 (12 600)	14.0^{sh} (112) 34.8^{sh} (12 300)	15.8 (683)	16.9 (740)	20.6^{sh} (814)	26.8 (9550)
2b	10.2^{sh} (20.9) 28.9 (14 800)	12.7 (254) 36.6 (15 200)	14.1^{sh} (123) 41.0 (21 300)	15.8 (649)	17.0 (722)	20.5^{sh} (797)	27.1^{sh} (12 600)
3b	9.88^{sh} (17.2) 35.2 (17 300)	12.7 (185) 39.4 (23 800)	14.1^{sh} (115)	15.8 (558)	16.9 (624)	20.4^{sh} (613)	27.1 (24 700)
4b	10.4 (15.2) 30.6^{sh} (7380)	12.8 (123) 33.2 (11 300)	14.2^{sh} (98.3) 37.2 (11 200)	15.9 (427)	17.2 (507)	21.4^{sh} (595)	26.7 (9100)
5b	10.3 (16.7) 28.5 (15 200)	12.8 (123) 34.1^{sh} (14 800)	14.2^{sh} (113) 37.3 (16 900)	15.8 (449)	17.2 (538)	21.2^{sh} (609)	26.7^{sh} (11 500)
6b	10.5 (17.5) 27.7 (23 200)	12.8 (126) 29.0^{sh} (20 300)	14.2^{sh} (115) 33.1 (17 500)	15.8 (461) 34.7 (17 700)	17.2 (551) 37.3 (29 600)	21.0^{sh} (612) 38.5^{sh} (26 500)	26.8^{sh} (21 600) 41.2 (23 100)
1c	9.50 (10.6)	12.9 (1.35)	16.3 (7.67)	27.4^{sh} (154)	31.6^{sh} (13 600)	33.0 (19 600)	37.9 (6140)

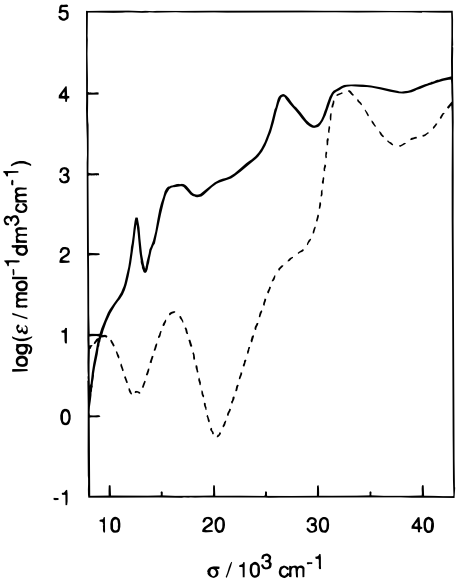

Figure 6. Absorption spectra of [Ni(acac)(tmen)(NIT2-py)]PF_6 (**1b**) (—) and [Ni(acac)(NO_3)(tmen)] (**1d**) (- - -) in CH_2Cl_2.

nonradical complexes as shown in Figures 5 and 6 and Table 5, it is noted that the electronic transitions in the ultraviolet region of the NIT2-py complexes exhibit the almost additive character of the nonradical (β-diketonato)nickel(II) complexes and NIT2-py and are not primarily influenced by the NIT2-py coordination.

5. Visible Absorption Bands: Charge-Transfer Transitions. In the region corresponding to the n−π* intraligand transitions of NIT-py or the second spin-allowed d−d $^3A_2 \rightarrow {}^3T_1$ band for the nonradical Ni(II) complexes, the visible absorption spectra of [Ni(β-diketonato)$_2$(NIT2-py)] and [Ni(β-diketonato)(tmen)(NIT2-py)]$^+$ complexes at (16.0−19.0) × 10^3 cm^{-1} give characteristics different from those of the ligand itself and the nonradical complexes. Two components were observed with a spacing of about 2000 cm^{-1} as a peak or a shoulder as shown in Figures 5 and 6 and Table 5. The positions of these components are shifted to higher frequency by substituting the methyl group for the phenyl group and/or for the trifluoromethyl group. Their intensities are much larger and the bandwidths are narrower than those of the ligand itself and the nonradical complexes. The molar absorption coefficients (ϵ) in this region are found to be influenced by the kinds of substituent groups on the β-diketonato coligands, e.g., decreasing at most by one-third upon substitution of the methyl group for the trifluoromethyl group. From these spectral behaviors, the visible bands may be assigned to neither the intraligand nor the d−d transitions but to the charge-transfer (MLCT) transitions as examined by the resonance Raman spectra below.

The resonance Raman spectra of [Ni(acac)$_2$(NIT2-py)]·CH_2Cl_2 in the solid state are shown in Figures 7 and 8. In these Raman spectra, for resonances in the region (16.0−19.0) × 10^3 cm^{-1}, significant intensity enhancement was observed, especially for the bands around 1520 and 1468 cm^{-1}, as shown in Figure 7. These two bands can be assigned to the stretching vibrations of the O−N═C moiety of the NIT2-py ligand. The remaining enhanced peaks from 614 to 660 cm^{-1} may be due to the M−O,N stretching. [Ni(acac)(tmen)(NIT2-py)]PF_6·$^1/_3CH_2Cl_2$ in the solid state and the related β-diketonato complexes give Raman spectra similar to that of the bis(acac) complex. Thus, the observed resonance enhancement of the Raman bands leads to the assignment of the (16−19) × 10^3 cm^{-1} components to the charge-transfer transition. This band is probably due to the metal t_{2g}-to-ligand SOMO π* (MLCT) transition as suggested by the blue shift in more polar solvents (from CH_2Cl_2 and CH_3CN to CH_3OH) and the following ligand field consideration.

There are three possible MLCT transitions: two $t_{2g} \rightarrow \pi^*$ transitions (doublet−doublet and quartet−quartet) and one $e_g \rightarrow \pi^*$ doublet−doublet transition (Scheme 1). In the doublet−doublet MLCT for octahedral Ni(II) complexes, the transition energy is estimated to be $30(\chi(\text{Ni}) - \chi(\text{NIT})) - {}^4/_3D$ for $E(t_{2g} \rightarrow \pi^*)$ and $30(\chi(\text{Ni}) - \chi(\text{NIT})) - \Delta + {}^5/_3D$ for $E(e_g \rightarrow \pi^*)$, where χ(Ni) and χ(NIT) refer to the optical electronegativities for nickel(II) and the NIT2-py ligand, respectively.[36,37] The

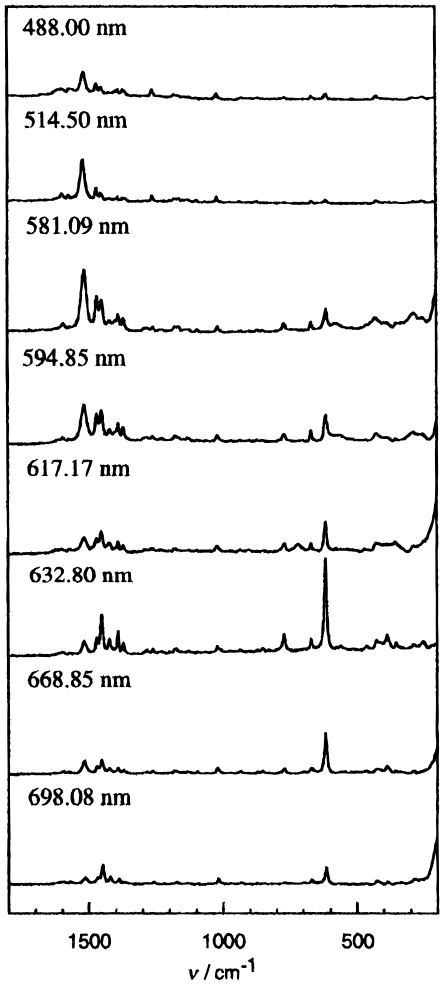

Figure 7. Resonance Raman spectra of $[Ni(acac)_2(NIT2\text{-}py)]\cdot CH_2Cl_2$ (**1a**) recorded by using 488.00, 514.50, 581.09, 594.85, 617.17, 632.80, 668.85, and 698.08 nm laser lines.

Scheme 1. MLCT Transitions

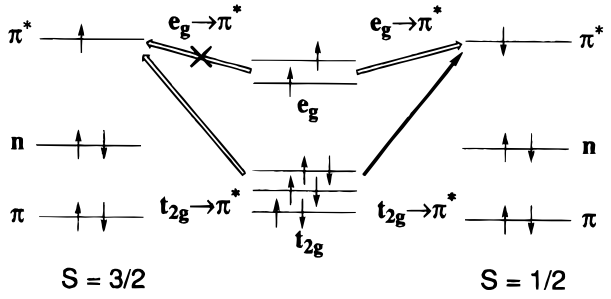

energy difference between two doublet−doublet MLCTs ($E(e_g \rightarrow \pi^*) - E(t_{2g} \rightarrow \pi^*)$) is given by $23.1B - \Delta$ ($D = 7.7B$)[37] and approximated to ca. 9300 and 8700 cm^{-1} for the bis(acac) and mono(acac) complexes, respectively, since Δ and B are estimated by using the first spin-allowed (Δ) and the spin-forbidden transition energies ($16B - 6B^2/\Delta$) (vide infra). Therefore, the lower energy MLCT components around (16.0−19.0) $\times$ 10^3 cm^{-1} and the shoulder around 25.0 $\times$ 10^3 cm^{-1} are due to the $t_{2g} \rightarrow \pi^*$ and the $e_g \rightarrow \pi^*$ MLCT transitions, respectively.

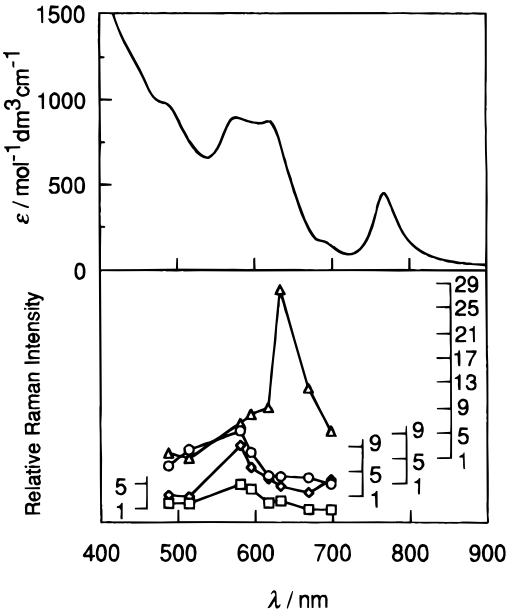

Figure 8. Excitation profiles of $[Ni(acac)_2(NIT2\text{-}py)]\cdot CH_2Cl_2$ (**1a**): 1517 cm^{-1} (○); 1468 cm^{-1} (□); 611 cm^{-1} (△); 286 cm^{-1} (◇).

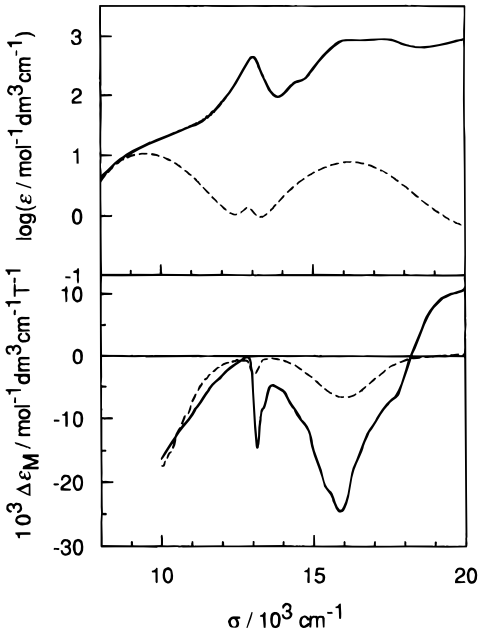

Figure 9. MCD spectra of $[Ni(acac)_2(NIT2\text{-}py)]$ (**1a**) (—) and $[Ni(acac)_2(tmen)]$ (**1c**) (- - -)in CH_2Cl_2.

6. Near-Infrared Absorption Spectra: Spin-Allowed and Spin-Forbidden d−d Transitions. The absorption spectral patterns around 10 $\times$ 10^3 cm^{-1} for two series of the NIT2-py complexes [Ni(β-diketonato)$_2$(NIT2-py)] and [Ni(β-diketonato)(tmen)(NIT2-py)]$^+$ are similar irrespective of the kinds of β-diketonates, as shown in Figures 5 and 6. The absorption band positions and intensities are almost the same as those of [Ni(β-diketonato)$_2$(tmen)] complexes in the first spin-allowed d−d ($^3A_2 \rightarrow {}^3T_2$) ligand field transition region around 10 $\times$ 10^3 cm^{-1}. This assignment is supported by the resemblance of the lowest frequency magnetic circular dichroism (MCD) band envelope in position and intensity of the radical complexes [Ni(β-diketonato)$_2$(NIT2-py)] and [Ni(β-diketonato)(tmen)(NIT2-py)]$^+$ to those of the nonradical complexes as shown in Figures 9 and 10. The absorption band positions of the bis(β-diketonato) NIT2-py complexes are always located at frequencies lower than those of the tmen (NIT2-py) complexes. It is seen that the ligand

(36) Lever, A. B. P. *Inorganic Spectroscopy*, 2nd ed.; Elsevier: Amsterdam, 1984; Chapter 5.
(37) Jørgensen, C. K. *Modern Aspects of Ligand Field Theory*; North-Holland Publishing Co.: Amsterdam, London, 1971; Chapter 21.

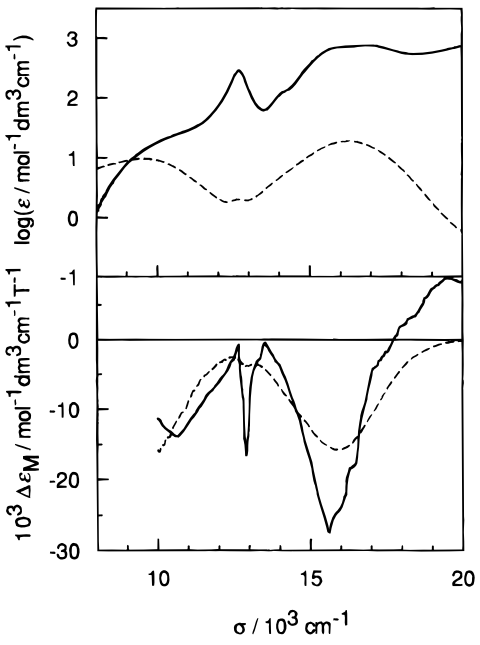

Figure 10. MCD spectra of [Ni(acac)(tmen)(NIT2-py)]PF_6 (**1b**) (—) and [Ni(acac)(NO_3)(tmen)] (**1d**) (- - -) in CH_2Cl_2.

field of tmen is stronger than that of the β-diketonates, as expected. Therefore, it is notable that the first spin-allowed d−d ($^3A_2 \rightarrow {}^3T_2$) transition in this region is not influenced by the NIT2-py radical, as shown in Table 5.

On the other hand, the intense bands around 13.0×10^3 cm^{-1} for [Ni(β-diketonato)$_2$(NIT2-py)] and [Ni(β-diketonato)(tmen)-(NIT2-py)]$^+$ complexes are observed in the region corresponding to the weak absorption peaks for the spin-forbidden $^3A_2 \rightarrow {}^1E$ d−d transitions of [Ni(β-diketonato)$_2$(tmen)] complexes. These band intensities (molar absorption coefficients ϵ) of the NIT2-py complexes are significantly enhanced about 100−350 times as compared with those of the corresponding nonradical complexes, as shown in Table 5. MCD bands of the radical complexes around 13.0×10^3 cm^{-1} are almost the same in position and bandwidth as those of the nonradical complexes, but the intensities ($\Delta\epsilon_M$) are several times larger than those of the nonradical complexes. Accordingly, this MCD behavior suggests that the absorption bands of the radical complexes around 13.0×10^3 cm^{-1} originate from the spin forbidden $^3A_2 \rightarrow {}^1E$ d−d transition.

The remarkable spectral behavior of the radical complexes around 13.0×10^3 cm^{-1} results from the exchange interaction between a paramagnetic nickel(II) ion and the NIT2-py radical, as discussed for semiquinone Cr(III) complexes.[19] The exchange-coupled ground state $^3A_2{}^2L_0$ consists of a doublet and a quartet, whereas the excited state $^1E^2L_0$ generates only a doublet, as shown in Figure 11. Therefore, the triplet−singlet spin-forbidden transitions of [Ni(β-diketonato)$_2$(NIT2-py)] and [Ni(β-diketonato)(tmen)(NIT2-py)]$^+$ complexes become formally spin-forbidden between the exchange-coupled doublets as a result of the breakdown of the $\Delta S = 0$ restriction. This assignment is supported by the enhancement of the intensity of the absorption band at 77 K as compared with that of the band at room temperature, which results from the Botlzmann depopulation of the quartet level in the ground state, in accordance with the antiferromagnetic interaction observed from the magnetic susceptibility measurements. The different behaviors of the magnetic and spectroscopic properties of two series of NIT2-py complexes with variation of the β-diketonates are accounted for in terms of the exchange mechanism for the intensity

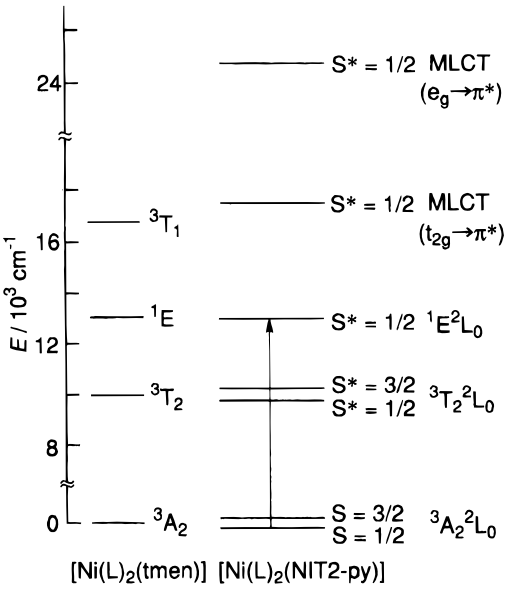

Figure 11. Energy levels of the spin-allowed and spin-forbidden d−d transitions in the β-diketonato Ni(II) complexes with NIT2-py.

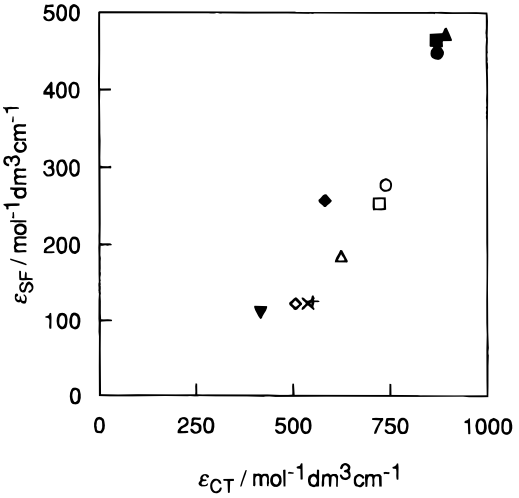

Figure 12. Plots of ϵ_{SF} vs ϵ_{MLCT} for the bis(β-diketonato) complexes **1a** (●), **2a** (■), **3a** (▲), **4a** (◆), and **5a** (▼) and for the mono(β-diketonato) complexes **1b** (○), **2b** (□), **3b** (△), **4b** (◇), **5b** (×), and **6b** (+).

enhancement of the NIT2-py complexes in the formally spin-forbidden d−d transition region as discussed below.

7. Correlation between the Absorption Intensity and the Magnetic Coupling Constant through the Substituent Effect. A large range of intensities (120−480 mol^{-1} dm^3 cm^{-1} for the molar absorption coefficients ϵ_{SF} at the maximum) in the formally spin-forbidden $^3A_2{}^2L_0 \rightarrow {}^1E^2L_0$ transition is observed for both series of the NIT2-py complexes in such a way that increasing intensity depends on the kinds of 1,3-substituents. The formally spin-forbidden band intensities increase with increasing ϵ_{CT} (550−910 mol^{-1} dm^3 cm^{-1})[38] at the maximum component in the MLCT transitions, as shown in Table 5 and Figure 12. Also, the ϵ_{SF} values increase with increasing absolute

(38) Though both the ϵ_{SF} and ϵ_{CT} reduced by the Boltzmann population at room temperature are necessarily corrected to those at very low temperature, this is ignored hereafter because the discussion is concerned with only the intensity ratio $\epsilon_{SF}/\epsilon_{CT}$, which is unchanged from high to low temperatures owing to the cancellation of the Boltzmann correction.

(39) Ferguson, J.; Guggenheim, H. J.; Tanabe, Y. *J. Phys. Soc. Jpn.* **1966**, *21*, 692.

J values for the bis(β-diketonato) and mono(β-diketonato)(tmen) NIT2-py complexes having respective β-diketonates, with some irregularities for the latter (CF_3-substituted-β-diketonato)(tmen) complexes. These facts strongly suggest that the formally spin-forbidden $^3A_2{}^2L_0 \rightarrow {}^1E^2L_0$ transition can attain the integrated intensity I_{SF} by borrowing the $t_{2g}-\pi^*$ SOMO charge-transfer integrated intensity I_{CT} through the exchange mechanism, which suggests some connection among the ϵ_{CT}, ϵ_{SF}, and *J* values in the multi-spin coupled systems.[19,39]

According to the formulation in terms of the exchange mechanism which is operative in the intensity enhancement of the $^3A_2 \rightarrow {}^1E$ transition as shown in eqs 1−3 , the product (eq

$$\frac{I_{SF}}{I_{CT}} = \left|\frac{h(CT)}{\Delta E_{CT}}\right|^2 \tag{1}$$

$$J \propto \frac{h(CT)^2}{\Delta E_{CT}} - K \tag{2}$$

$$J \propto \frac{I_{SF}}{I_{CT}}\Delta E_{CT} = \frac{\epsilon_{SF}\Delta^{SF}_{1/2}}{\epsilon_{CT}\Delta^{CT}_{1/2}}\Delta E_{CT} \approx \frac{\epsilon_{SF}}{\epsilon_{CT}}\Delta E_{CT} \tag{3}$$

3) of the integrated intensity ratio I_{SF}/I_{CT} and the charge-transfer transition energy ΔE_{CT} is related to the exchange coupling constant *J* through the charge-transfer integral $h(CT)$ in eqs 1 and 2 when the exchange integral *K* is neglected.[19,39]

As in eq 3, the integrated intensity *I* may be approximated by the product of the molar absorption coefficient (ϵ) and the half-bandwidth ($\Delta_{1/2}$). Actually, since the $\Delta_{1/2}$ values of the MLCT components are similar to those of the formally spin-forbidden bands, the ratios of $\epsilon_{SF}/\epsilon_{CT}$ are taken for simplicity instead of I_{SF}/I_{CT} in the following discussion. *J* values in eq 3 should correspond thoroughly to antiferromagnetic exchange coupling constants J_{AF} because the doublet−doublet MLCT considered is concerned with the stabilization of the doublet level in the ground state through the exchange coupling.[40] If the J_{obsd} values obtained from the magnetic susceptibility measurements were due to antiferromagnetic couplings, a plot of the right member of eq 3 against the J_{obsd} values would give a linear relation. This is approximately realized for the J_{obsd} values of the bis(β-diketonato) complexes and the methyl- and phenyl-substituted mono(β-diketonato)(tmen) complexes but not for those of the latter trifluoromethyl-substituted complexes, as shown in Figure 13. The decrease in the values for the right member in eq 3 upon changing one of two respective β-diketonates for tmen reflects a decrease in the antiferromagnetic interaction (J_{AF}) as found for the J_{obsd} values. The variation of the J_{obsd} values upon substituting the methyl group of acac with phenyl and trifluoromethyl groups suggests the substituent effect for the 1- and 3-positions of the β-diketonates on the J_{AF} value. The substituent effect is examined quantitatively by introducing the Hammett constant σ_m,[41] since the electronic influence on the Ni(II) ion at the meta position with respect to the 1- and 3-substitution in the β-diketonates is considered to play an important role in the magnetic interactions with NIT2-py. Then, a plot of the right member of eq 3 against $\sum\sigma_m$[42] (the sum for the substituents in the complexes) results in a linear correlation for the mono(β-diketonato)(NIT2-py) complexes and in a nearly linear one for the bis(β-diketonato)(NIT2-py) complexes, as

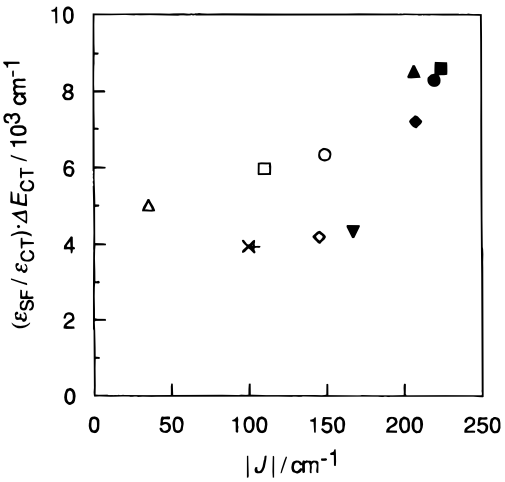

Figure 13. Plots of $(\epsilon_{SF}/\epsilon_{MLCT})\cdot\Delta E_{MLCT}$ vs $|J|$ for the bis(β-diketonato) complexes **1a** (●), **2a** (■), **3a** (▲), **4a** (◆), and **5a** (▼) and for the mono(β-diketonato) complexes **1b** (○), **2b** (□), **3b** (△), **4b** (◇), **5b** (×), and **6b** (+).

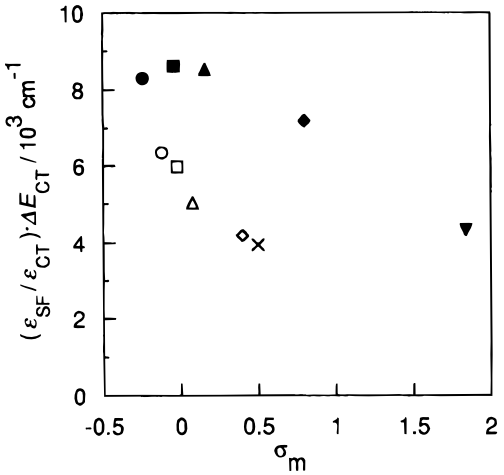

Figure 14. Plots of $(\epsilon_{SF}/\epsilon_{MLCT})\cdot\Delta E_{MLCT}$ vs σ_m for the bis(β-diketonato) complexes **1a** (●), **2a** (■), **3a** (▲), **4a** (◆), **5a** (▼) and for the mono-(β-diketonato) complexes **1b** (○), **2b** (□), **3b** (△), **4b** (◇), and **5b** (×).

shown in Figure 14. That is, the larger the electron-withdrawing capability of the substituents, the smaller the right member[43] of eq 3 or the antiferromagentic coupling is. This relation is seen for the J_{obsd} values of the bis(β-diketonato) complexes, while there are some discrepancies for the J_{obsd} values of the mono(β-diketonato) complexes. This is accounted for as follows. The J_{obsd} values represent the sum of an antiferromagnetic coupling constant J_{AF}, attributed to a doublet−doublet MLCT, and a ferromagnetic coupling constant J_F, which may be attributed to the stabilization of the quartet level in the ground state through a strong interaction with the quartet MLCT, as in eq 4. Therefore, the magnetic interactions of the bis(β-

$$J_{obsd} = J_{AF} + J_F \tag{4}$$

diketonato) complexes are mainly attributed to the antiferromagnetic coupling of the first term (J_{AF}) of eq 4, whereas the difference in the J_{obsd} values observed especially for the CF_3 substitution in the mono(β-diketonato) complexes may arise

(40) Kahn, O. *Molecular Magnetism*; VCH: Berlin, 1993; Chapter 8.
(41) Linert, W.; Taha, A. *J. Chem. Soc., Dalton Trans*. **1994**, 1091.
(42) Gordon, A. J.; Ford, R. A. *The Chemist's Companion*; John Wiley & Sons: New York, 1972.

(43) The absolute values of the ordinate seem to be more than an order of magnitude over the expected ones. This is because the MLCT intensities are underestimated, only one of a few components with similar bandwidths being taken into consideration for simplicity and because of difficulty in performing the curve deconvolution.

from the variation of the ferromagnetic contribution J_F in addition to that of the antiferromagnetic contribution J_{AF} with change of the β-diketonato coligands.

Conclusions

For two series of newly synthesized and characterized bis-(β-diketonato)- and (β-diketonato)(tmen) NIT2-py nickel(II) complexes, there is a significant relation between the intensities of the formally spin-forbidden bands and those of the new MLCT components on the basis of the observed magnetic coupling constants. This is interpreted by using the exchange mechanism in such a way that the enhanced intensities in the formally spin-forbidden d−d transitions between the spin-coupled doublets are acquired from those of the MLCT through the antiferromagnetic coupling and are correlated with each other in terms of the substituent effects or the Hammett constants of 1,3-substituents in the β-diketonate coligands.

Acknowledgment. We gratefully thank Prof. Wasuke Mori and Dr. Satoshi Takamizawa of Kanagawa University for measuring the magnetic susceptibilities. We acknowledge support of this research by a Grant-in-Aid for Scientific Research (No.06453049) from the Ministry of Education, Science and Culture of Japan.

Supporting Information Available: X-ray crystallographic files, in CIF format, for **1b**, **2b**, and **5b**, Figures S1−S8 ($\chi_M T$ vs T plots for **2a**, **3a**, **4a**, **5a**, **6a**, **2b**, **3b**, **4b**, and **5b**), Figures S9−S16 (absorption and MCD spectra for **2a**, **3a**, **4a**, **5a**, **2b**, **3b**, **4b**, and **5b**), and Table S1 (absorption spectral data for **1c**, **2c**, **3c**, **4c**, **5c**, **1d**, **2d**, **3d**, **4d**, **5d**, and **6d**). This material is available free of charge on the Internet at http://pubs.acs.org.

IC981283N